# Researches on the Fatigue under Consideration of the Phenomenon of Elastic Hysteresis

AUTHOR(S):

KAWAMOTO, Minoru; NISHIOKA, Kunio

# Researches on the Fatigue under Consideration of the Phenomenon of Elastic Hysteresis

By

Minoru KAWAMOTO and Kunio NISHIOKA

Department of Mechanical Engineering

(Received November, 1954)

## Introduction

In the conventional researches on the fatigue of metals, the reversed stress at the surface of specimens has been calculated by the theory of elasticity. For the purpose of application of the results of the fatigue tests to practical designs, the above consideration is sufficient. However, if we purport to clarify the essential character of fatigue and to give a satisfactory explanation to various experimental results on fatigue, the procedure that treats it as the elastic material is not proper.

The phenomenon of the so-called "fatigue", in brief, is the fracture caused by very minute slips which occur in the materials due to the reversed stress and gradually make the material brittle. Consequently, since the slip does occur, it is a matter of course that there exists no linear relation between stress and strain as considered in the theory of elasticity, and some amount of irreversible work is expended in the form of internal friction.

Many a fatigue test have been performed in the past to obtain design data for the machine parts, and the essential studies have also been carried out so that there are today sufficient number of results that shows that the relation between stress and strain during the fatigue tests is not linear. For example, Bairstow[1], Mason[2] and the others found that when a material is subjected to the alternating stress beyond a certain level, the phenomenon of elastic hysteresis appears between stress and strain. Also, Nagasawa[3] carried out a test to obtain the relation between the magnitude of elastic hysteresis loop and the reversed stress for the purpose of rapid determination of the fatigue limit, and had found that the loop appears even at a considerably low stress below the fatigue limit. Dorey[4] had also obtained the elastic hysteresis loop in connection with his study to determine the superiority of crank shaft material against the reversed torsion. Lazan and Wu[5] have recently investigated the elastic hysteresis loop considerably in detail.

The above the cases in which the elastic hysteresis loop caused by the reversed stress was directly sought for by experiments; besides, there are many investigations conducted that indirectly proves the fact that the phenomenon of elastic hysteresis appears even under the reversed stress which is lower than the fatigue limit. There are many instances in experiments concerning the measurement of damping capacity. Brophy[6], for example, had found that some relation exists between the damping capacity and the notch sensitivity. Also in the experiments[7] in which the rapid determination of fatigue limit was measured by the temperature-rise of specimen, a remarkable temperature-rise was recognized when the reversed stress exceeded a certain stress level. Again, Kikukawa[8], measuring the deflection of specimen in his rotating bending tests, had discovered that the deflection of specimen increases with the number of stress cycles at stress levels below the fatigue limit. And again, Nishihara and Kawamoto[9] had dissected the specimen after the fatigue test and by corroding the dissected surface, had detected the part that was fatigued. As the result, it was recognized the fatigued portion penetrated considerably deep into the center of specimen even at the fatigue limit.

The above experimental results are indirect, yet they go to show the fact that the elastic hysteresis loop gradually increases owing to the fatigue of material. An important fact at this point is the fact that the elastic hysteresis loop thus appears and the reversed stress, which loses a direct relation between stress and strain, is lower than the fatigue limit.

Taking the above facts into consideration, it is a matter of course that there are many incomprehensible instances among various fatigue phenomena because the previous consideration has been based upon a supposition that there is a linear relation between stress and strain.

It seems important to take the phenomenon of elastic hysteresis into consideration in explaining various problems such as the influence of the shape of cross section of specimen upon the fatigue limit-the experiments of which have recently been begun — or the problem of the relation between the form factor (stress concentration factor) and the notch factor (fatigue limit reduction factor) — which cannot be said to have been clarified as yet. This consideration is necessary in an endeavor to explain various fatigue phenomena in more detail than it is done today.

From the above consideration, this study has been conducted to show how the distribution of reversed stress in the specimen obtained in the fatigue test should be treated, to obtain information regarding the relative magnitude of the effect of shape of cross section on flexural fatigue strength and the relation between the form factor and notch factor, and to analyze these data basing upon the phenomenon of elastic hysteresis. The results derived theoretically showed good coincidence with the experimental results.

## Chapter 1. Relation between stress and strain on the metallic material subjected to the reversed stress and the condition of fatigue limit

### 1. Introduction

As has been mentioned previously, in the metal subjected to the reversed stress over a certain critical level, the phenomenon of elastic hysteresis appears, and that portion can be detected by a corrosion method and is called as the fatigued portion. In this chapter we shall express the phenomenon of elastic hysteresis by a simple equation and consider at the same time the condition of fatigue limit.

### 2. Stress-strain relation under the reversed stress in the metallic material

The stress-strain relation in the metals subjected to the reversed stress has been studied by Bairstow[1], Mason[2], Dorey[4] and the others as mentioned in the Introduction. An elastic hysteresis loop drawn on a basis of their experimental results is shown schematically in Fig. 1 with ABCD, where the stressing is in the direction of A→B→C→D→A. It is known from these experimental results that the character of elastic hysteresis loop is as follows:

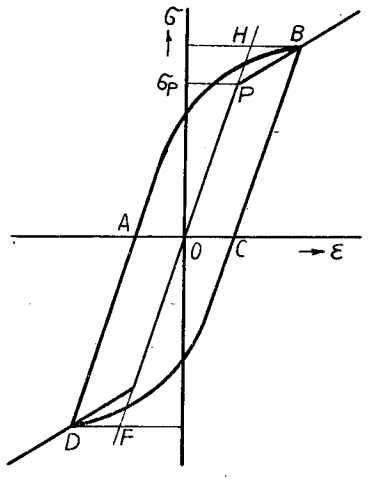


Fig. 1. Schematic diagram of elastic hysteresis loop.

(1) Unless the reversed stress is much greater than the fatigue limit, the width of loop, AC, in Fig. 1 increases drastically at the early stage of stress repetitions and then the rate of increase diminishes gradually. The increase ceases perfectly after a certain number of stress repetitions is reached and it does not increase however the number of stress repetition is increased. The range in which the width of loop become equilibrium is from several thousands to ten thousands in most cases.

(2) The lines BC and DA, in Fig. 1, which illustrate the relation between stress and strain while the stress is being decreased are expressed by straight lines parallel to the line FOH which represents a relation between stress and strain in the perfectly elastic material prior to fatigue tests.

(3) The width of loop, AC, in the state of equilibrium reached after some numbers of stress repetitions, is proportional to the difference between a reversed stress at the time, $\sigma$, and the stress $\sigma_p$, at which such loop begins to appear. Accordingly, in Fig. 1, when tests were carried out at various levels of the reversed stress and the

elastic hysteresis loop become steady, each extreme point of the loop corresponding to the point B in Fig. 1 falls on a straight line as shown in the figure with PB.

Taking the above characteristics of elastic hysteresis loop into consideration, the stress-strain relation at the portion PB can be obtained by;

$$\varepsilon = \frac{1}{E'}(\sigma - \sigma_p) + \frac{\sigma}{E} \qquad (1) \qquad \text{or} \qquad \sigma = \frac{E'\varepsilon + \sigma_p}{1 + E'/E}, \qquad (1')$$

where $E$ is the tangent of the line OP and the so-called elastic modulus, while $E'$ is a constant calculated from the following equation,

$$\frac{1}{E'} = \frac{1}{E''} - \frac{1}{E}, \qquad (2)$$

in which $E''$ is taken as a tangent of the line PB.

### 3. Condition of the fatigue limit

Considering many experimental results mentioned in the Introduction, it is clear that the elastic hysteresis loop appears even at the reversed stress below the fatigue limit $\sigma_w$ and, consequently, the fact that $\sigma_p$ in Fig. 1 is lower than $\sigma_w$ is understood. Therefore, putting

$$\sigma_p = \kappa\sigma_w \quad (\kappa < 1), \qquad (3)$$

the strain at the fatigue limit, $\varepsilon_w$, becomes as follows;

$$\varepsilon_w = \left\{1 + \frac{E}{E'}(1-\kappa)\right\}\frac{\sigma_w}{E}. \qquad (4)$$

Generally, the consideration for fatigue phenomena in the past has been made on the basis of the reversed stress calculated from the theory of elasticity; however, the authors, in dealing with various instances hereafter in this paper, shall consider the fatigue limit as the limit which makes the maximum strain equal to $\varepsilon_w$ shown in Eq. (4). In other words, Eq. (4) gives a condition of fatigue limit in the case of normal stress. In the case of uniform stress distribution, however, no distinction is necessary because there is no difference caused on stress by the appearance of elastic hysteresis loop whether $\sigma_w$ is given as in the past or as the authors do with $\varepsilon_w$. On the other hand, in the case of non-uniform stress distribution, it becomes necessary to give the fatigue limit with $\varepsilon_w$ as will be described later.

The above discussion has clarified the case of uniform distribution of normal stress, and we shall next consider the case of uniform distribution of shearing stress. In order to seek the elastic hysteresis loop under uniform shearing stress distribution, we must use extremely thin-walled tubular specimens. It is a practical impossibility, so let us suppose that such a test could have been done and the elastic hysteresis loop had been obtained. Then the loop in this case is conceivable to have

the same characteristics as that under normal stresses. Therefore, the relation between stress and strain and the condition of fatigue limit in this case become, in accordance with (1′) and (4), as follows;

$$\tau = \frac{G'\gamma + \tau_p}{1+G'/G}, \tag{5}$$

$$\gamma_w = \left\{1+\frac{G}{G'}(1-\kappa)\right\}\frac{\tau_w}{G}, \tag{6}$$

where $\tau_p$ and $G'$ are the constants corresponding to $\sigma_p$ and $E'$ in the case of normal stress, while $\tau_w$ is the torsional fatigue limit of the thin-walled tubular specimen and $\gamma_w$ the shearing strain corresponding to the case.

In the above, the stress-strain relation under uniform stress distribution and the condition of fatigue limit have been presented with equations of simple form. The magnitudes of $E$, $E'$, $G$, $G'$, and $\kappa$ in those equations will be known if the experiments in which the elastic hysteresis loop are formed are carried out at various levels of the reversed stress. However, since the authors did not perform those experiments, the values will be inferred from those experimental results obtained by the others.

## 4. Values of $E/E'$, $G/G'$ and $\kappa$

The values of $E$, $G$ can be found from the static tests, but the values of $E'$, $G'$ and $\kappa$ must depend upon the reversed stress tests. In the equation hereafter they will never enter individually as $E'$ or $G'$ but always in the form of $E/E'$ or $G/G'$ and, we shall attempt to obtain those values from the experimental results which have made in the past.

Mason carried out the tests with the solid and tubular specimens of 0.12% C steel under reversed bending and reversed torsion, and obtained the elastic hysteresis loop for each case. Based on these results, the values of $E/E'$, $G/G'$ and $\kappa$ become approximately as follows;

$$\left.\begin{aligned} E/E' &= 2\sim4 \\ G/G' &= 3\sim6 \\ \kappa &= 0.9 \end{aligned}\right\}. \tag{7}$$

While Nishihara and Kawamoto[9] conducted their experiments on reversed tension-compression and rotating bending with the 0.09% C steel and discovered that, although the fatigue limit under reversed tension-compression was 15.68 kg/mm², the fatigued portion began to appear for the first time at 14.16 kg/mm² of rotating bending stress. Then from Eq. (3),

$$\kappa = \frac{\sigma_p}{\sigma_w} = \frac{14.16}{15.68} \simeq 0.9 .$$

Also, from the elastic hysteresis loop obtained by Nagasawa[3] with 0.9% C steel under cantilever-rotating bending tests, $\kappa$ and $E/E'$ become 0.8 and 4 respectively.

Considering the above experimental results, for commercial carbon steels, the values of $E/E'$, $G/G'$ and $\kappa$ are considered as being in the following ranges,

$$\left.\begin{aligned} E/E' &= 0\sim 4 \\ G/G' &= 0\sim 8 \\ \kappa &= 0.8\sim 0.9 \end{aligned}\right\}. \tag{8}$$

For the convenience of the treatment, $\kappa$ will be taken as a constant value of 0.9 throughout this investigation, therefore, the values of $E/E'$ and $G/G'$ may in some instances exceed those ranges. Within those ranges, generally speaking, it is considered that the values of $E/E'$ or $G/G'$ decrease with the increase of carbon content or in the materials which have become brittle owing to heat treatment such as quenching. In consideration of the past experimental results, we do not know those values for the materials, then the appropriate value within the range shown in (8) will be taken in accordance with each case.

### 5. Conclusions

In this chapter, the stress-strain relation during fatigue tests was represented with simple expressions from the previous experimental results, and the condition of the fatigue limit under uniform stress distribution was obtained.

## Chapter 2. The Effect of Shape of Cross Section of Specimen on the Fatigue Limit

### 1. Introduction

It has been known well by many a previous investigation that the fatigue limit is influenced to a considerable extent by the size of specimen even for the same material. It is also known by a few studies made that the shape of cross section also influences the fatigue properties of a uniform bar. Consequently, although the literatures to be cited are very little, we shall survey those few results.

Moore[10], comparing the degree of fatigue limit under flexural bending between the round cross section and rectangular cross section, had obtained a result that the fatigue limit of the latter was 81% of the former. Also Gough[11] demonstrated that the torsional fatigue limit for the tubular specimens was about 10% less than the one for the solid specimens. In the recent tests by Fuller and Oberg[12] under flexural bending and rotating one, it has been observed that the rectangular specimen exhibited lower fatigue limit than that of the round specimen. Recently Dolan, McClow and Craig[13] have tested with specimens of four kinds of cross section and found that

the round specimens developed higher fatigue limits than those of the other three kinds of specimens.

It is obvious from the above experimental results that the fatigue limit is influenced by the shape of cross section of specimen. And the possible factors causing a shape of cross section to influence the fatigue limit have been considered as follows; the difference of type of testing machine used, the difference in the relative amount of defects in the material which cause the fatigue to appear, and the fact that it is considered that the fatigue limit is influenced by the shape of cross section by the same reason that the bending yield point is influenced by the shape of cross section. There are others who considered this point by taking an average value of stress between the surface and a certain depth. However, it seems that none of them can present a thoroughly appropriate explanation on this problem. Hereupon, the authors considered that the difference of the fatigue limits due to the shape of cross section depends upon the phenomenon of elastic hysteresis during the fatigue tests, and theoretically studied the differences among the fatigue limits caused by various shapes of cross section. And, in order to check for the appropriateness of such a conception, a series of tests were performed by using the specimens with the round, rectangular, I-shape, cross-shape and tubular cross sections under flexural bending, and also comparison were made with the experimental results obtained by other investigators.

## 2. Theoretical consideration of the fatigue limit caused by various shapes of cross section of specimens

In chapter 1, we have discussed on the existence of the phenomenon of elastic hysteresis between stress and strain even at the fatigue limit, and also described the stress-strain relation of that instance and the condition of fatigue has been made clear. In the subsequent discussion, the fatigue caused by various shapes of cross section will be theoretically considered on the basis of the abovementioned conception.

Since the same consideration can be applied to the other cases, the flexural bending fatigue limit of rectangular specimens, which is most convenient for the explanation, will be discussed.

When a rectangular specimen is subjected to a nominal reversed bending stress $\sigma_1$, which is greater than the tension-compression fatigue limit $\sigma_w$, the phenomenon of elastic hysteresis appears between stress and strain near the surface of specimen and the material becomes fatigued, and the stress that functions there becomes smaller than it appears to be. In usual tests performed under constant bending moment, the stress in the inner portion must increase elastically in order to supplement the decrease of stress near the surface, consequently the deflection of specimen becomes larger than at the beginning of test.

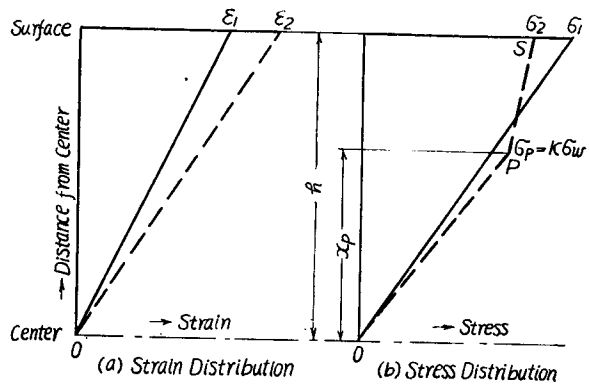


Fig. 2. The strain and stress distributions in the specimen.

Fig. 2 illustrates the abovementioned condition and (a) and (b) show the distributions of strain and stress respectively. In both (a) and (b), the full line represents the distribution at the beginning of test and the dotted line, the distribution at a state in which the elastic hysteresis loop becomes steady after some number of stress repetitions are given. In considering the state represented by the dotted line, the strain distribution must be linear as at the beginning of test from Bernoulli's hypothesis of maintenance of plane. In the stress distribution, on the other hand, the stresses near the surface decrease as mentioned above from $\sigma_1$ to $\sigma_2$ and finally assume the forms of distribution which are shown with the two direct lines PS and OP. In which, PS corresponds to the stress distribution in the fatigued portion, while OP, the stress distribution in the elastic portion. Further, since such a stress distribution occurs in the early stage of stress repetitions, it may be considered that, even if $\sigma_1$ is greater than $\sigma_w$, no fatigue failure occurs so long as $\sigma_2$ is less than $\sigma_w$. In other words, the bending fatigue limit conventionally considered can be said to be the value of $\sigma_1$ when $\sigma_2$ is just equal to $\sigma_w$. Since the strain $\varepsilon_w$ at the time $\sigma_2$ becomes equal to $\sigma_w$ can be obtained from Eq. (4), the so-called fatigue limit is obtained from the condition under which the surface strain becomes equal to $\varepsilon_w$. Hence, putting $\varepsilon_w$ as the surface strain, the internal strain distribution is obtained from the abovementioned plane maintenance hypothesis; and the internal stress distribution can be obtained by applying Eq. (1′) and the elastic relation $\sigma=E\varepsilon$ on the fatigue portion and the elastic portion. By dividing the bending moment obtained from those stress distributions by the sectional coefficient, the so-called bending fatigue limit can be obtained.

The following equations represent the fatigue limits for various shapes of cross section obtained by the above method.

$$\sigma'_{w\blacksquare}=\left[1+\frac{1}{2}\frac{\kappa}{1+\frac{E'}{E}}-\frac{1}{2}\frac{1}{1+\frac{E'}{E}}\frac{\kappa^3}{\left\{1+\frac{E}{E'}(1-\kappa)\right\}^2}\right]\sigma_w \tag{9}$$

$$\sigma'_{w\bullet}=\left[\frac{1+\frac{E}{E'}(1-\kappa)}{1+\frac{E}{E'}}+\frac{2}{\pi}\frac{1+\frac{E}{E'}(1-\kappa)}{1+\frac{E'}{E}}\sin^{-1}\frac{\kappa}{1+\frac{E}{E'}(1-\kappa)}+\frac{4}{3\pi}\frac{\kappa}{1+\frac{E'}{E}}\left\{1-\left(\frac{\kappa}{1+\frac{E}{E'}(1-\kappa)}\right)^2\right\}^{\frac{3}{2}}\right.$$

$$+\frac{2}{\pi}\frac{\kappa}{1+\frac{E'}{E}}\left\{1-\left(\frac{\kappa}{1+\frac{E}{E'}(1-\kappa)}\right)^2\right\}^{\frac{1}{2}}\Bigg]\sigma_w \tag{10}$$

$$\sigma'_{wI}=\frac{1}{1-(1-\eta)\xi^3}\left[\frac{\sigma'_{w\blacksquare}}{\sigma_w}-(1-\eta)\xi^3\left\{1+\frac{E}{E'}(1-\kappa)\right\}\right]\sigma_w \tag{11}$$

$$\sigma'_{w+}=\frac{1}{\eta+(1-\eta)\xi^3}\left[(1-\eta)\xi^3\left\{1+\frac{E}{E'}(1-\kappa)\right\}+\eta\frac{\sigma'_{w\blacksquare}}{\sigma_w}\right]\sigma_w \tag{12}$$

$$\sigma'_{w\bigcirc}=\frac{1}{1-\gamma^4}\Bigg[\frac{\sigma'_{w\bullet}}{\sigma_w}-\Bigg[\frac{1+\frac{E}{E'}(1-\kappa)}{1+\frac{E}{E'}}\gamma^4+\frac{2}{\pi}\frac{1+\frac{E}{E'}(1-\kappa)}{1+\frac{E'}{E}}\gamma^4\sin^{-1}\frac{\kappa}{\left\{1+\frac{E}{E'}(1-\kappa)\right\}\gamma}$$

$$+\frac{4}{3\pi}\frac{\kappa}{1+\frac{E'}{E}}\left\{\gamma^2-\left(\frac{\kappa}{1+\frac{E}{E'}(1-\kappa)}\right)^2\right\}^{\frac{3}{2}}+\frac{2}{\pi}\frac{\kappa}{1+\frac{E'}{E}}\gamma^2\left\{\xi^2-\left(\frac{\kappa}{1+\frac{E}{E'}(1-\kappa)}\right)^2\right\}^{\frac{1}{2}}\Bigg]\Bigg]\sigma_w. \tag{13}$$

In these equations the symbols of $\sigma'_{w\blacksquare}$, $\sigma'_{w\bullet}$, $\sigma'_{wI}$, $\sigma'_{w+}$, and $\sigma'_{w\bigcirc}$ denote the respective fatigue limits for rectangular, round, I-shape, cross-shape and tubular specimens. Also $\gamma$ in Eq. (13) is the ratio of inner diameter to outer diameter in the case of tubular specimens; while $\xi$ and $\eta$ in Eqs. (11) and (12) are constants as shown in Fig. 3. In the cases of I-shape, cross-shape and tubular cross sections, the above equations will vary when those values of $\xi$ or $\gamma$ exceeds a certain limit, but the equations applicable for specimens to be used in the later experiments are represented here. For the purpose of obtaining the bending fatigue limits from those equations, it suffices to find the values of $E/E'$ and $\kappa$ since the values of $\xi$, $\eta$ or $\gamma$ are determined by the shape of cross section of specimens.

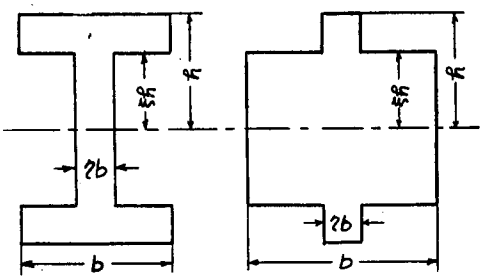

Fig. 3. Dimensions of I-shape and cross-shape cross sections.

Heretofore the fatigue limits for flexural bending has been discussed and we shall next consider the reversed torsional fatigue limits of solid and tubular specimens. The procedure here is quite similar to that in the foregoing discussions with slight variations: use Eq. (5) as the equation for stress and strain and Eq. (6) expressing the strain at the fatigue limit in place of Eq. (1) and (4) respectively.

Applying the torsional fatigue limits $\tau_w$ for the thin-walled tube to obtain $\tau_{w\bullet}$ and $\tau_{w\bigcirc}$ for the solid specimen and the tubular specimens of optional wall thickness, we have the followings,

$$\tau_{w\bullet}=\left[1+\frac{1}{3}\frac{\kappa}{1+\frac{G'}{G}}-\frac{1}{3}\frac{\kappa^4}{1+\frac{G'}{G}}\frac{1}{\left\{1+\frac{G}{G'}(1-\kappa)\right\}^3}\right]\tau_w \tag{14}$$

$$\tau_{w\bigcirc}=\left\{1+\frac{\kappa}{1+\frac{G'}{G}}\left(\frac{4}{3}\frac{1-\gamma^3}{1-\gamma^4}-1\right)\right\}\tau_w, \quad \text{for} \quad \gamma\geq\frac{\kappa\tau_w}{G\gamma_w} \tag{15}$$

$$\tau_{w\bigcirc}=\frac{1}{1-\gamma^4}\left[\frac{\tau_{w\bullet}}{\tau_w}-\gamma^4\left\{1+\frac{G}{G'}(1-\kappa)\right\}\right]\tau_w, \quad \text{for} \quad \gamma\leq\frac{\kappa\tau_w}{G\gamma_w} \tag{16}$$

in which $\tau_w$ is the torsional fatigue limit of idealy thin-walled tubular specimen and $\gamma$ in Eqs. (15) and (16) denotes the ratio of inner diameter to outer diameter in tubular specimens. Eq. (15) is applicable in the case when the entire interior of specimens is fatigued, while Eq. (16) is applicable when both the elastic portion and the fatigued portion concurrently exist. In other words, the former equation is applicable for comparatively thin-walled specimens and the latter, for thick-walled specimens.

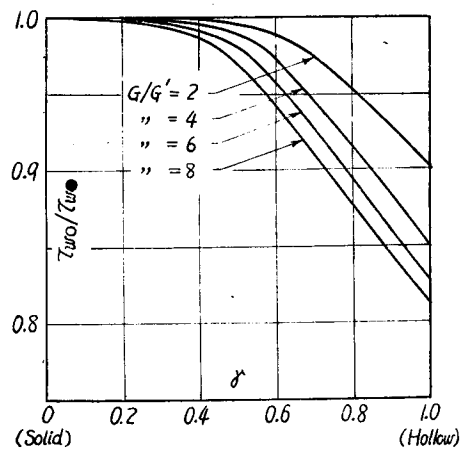


Fig. 4. Relation between the wall thickness and $\tau_{w\bigcirc}/\tau_{w\bullet}$ ($\kappa$=0.9).

Fig. 4 illustrates, based upon the torsional fatigue limit $\tau_{w\bullet}$ of solid specimen, how the torsional fatigue limits varies as the thickness of wall of tubular specimens become gradually thinner. Here, $\kappa$=0.9 has been applied and $G/G'$ has been varied between 2–8.

As seen in the figure, in tubular specimens, the thinner the thickness of wall becomes, the lesser becomes the fatigue limit. And such a tendency is more remarkable for the greater values of $G/G'$, that is, for the material that yields the larger elastic hysteresis loop.

Heretofore, it has been theoretically clarified how and to what extent the fatigue limit under flexural bending or reversed torsion is influenced by the shape of cross section of specimen.

## 3. Experimental results and the consideration

### 3.1 Experimental results by the authors and the consideration

In order to verify the appropriateness of the theoretical consideration discussed in the foregone chapter, the authors made a comparison of the fatigue limits on five specimens each having a different shape of cross sections : namely, round, rectangular, I-shape, cross-shape and tubular. The adaption of specimens having such a special shape of cross section as I-shape or cross-shape to this experiment was for the purpose of convenience in comparing and studying the results of the authors' conception with those of prevalent conception.

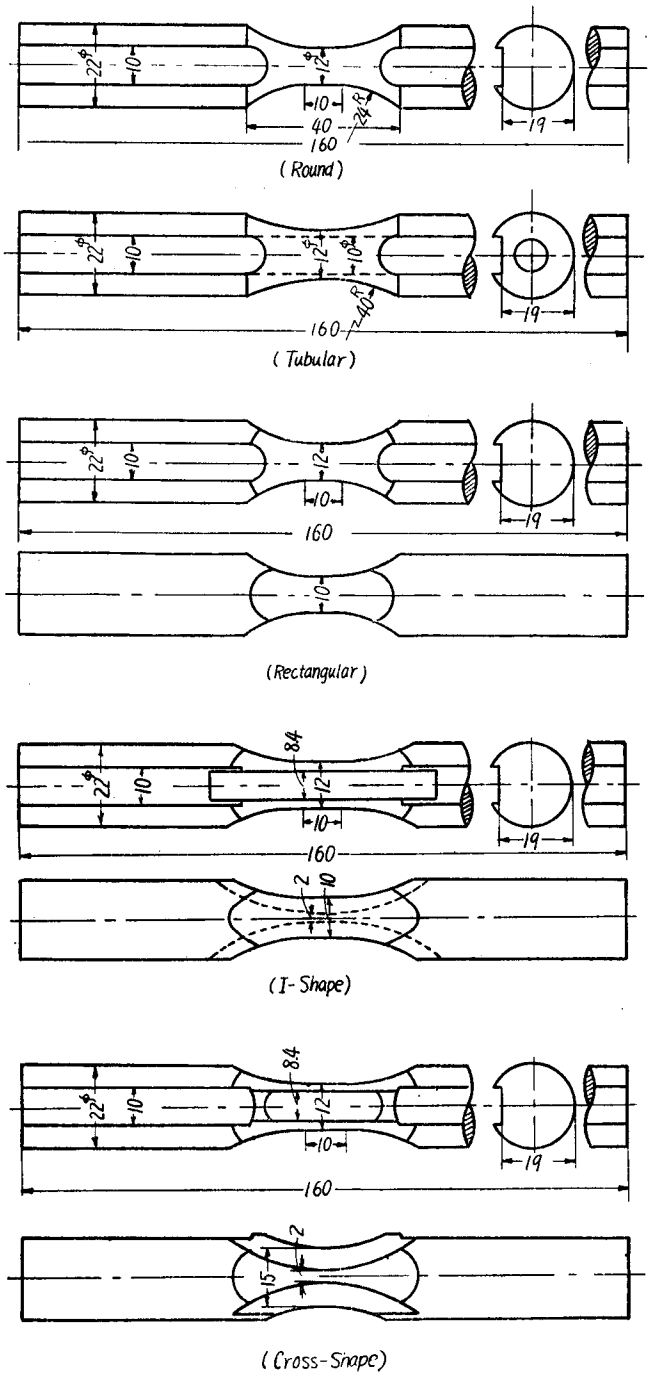


Fig. 5. Shapes and dimensions of test specimens.

Table 1. Chemical composition of materials (%)

| Mark | C | Mn | Si | P | S |
|---|---|---|---|---|---|
| 5695 | 0.10 | 0.50 | 0.14 | 0.033 | 0.040 |
| 251 | 0.57 | 0.32 | 0.31 | 0.022 | 0.022 |

The specimens used in this tests are of two kinds of carbon steel: the mild steel and hard steel; and their chemical compositions and mechanical properties are as listed in Tables 1 and 2.

Table 2. Heat treatment and mechanical properties of materials

| Mark | Heat Treatment | Upper yield point, kg/mm² | Lower Yield Point, kg/mm² | Tensile strength, kg/mm² | Breaking strength on Final Area, kg/mm² | Elongation, % | Reduction of Area, % | Hardness, Shore |
|---|---|---|---|---|---|---|---|---|
| 5695 | Heated in vacuum at 910°C for 1hr., then cooled in furnace. | 23.6 | 19.4 | 38.6 | 72.5 | 41.5 | 64.4 | 17.5 |
| 251 | Heated in vacuum at 810°C for 1hr., then cooled in furnace. | 37.0 | 33.7 | 63.4 | 96.0 | 21.1 | 46.1 | 26.0 |

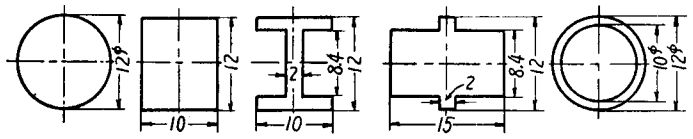


Fig. 6. Shapes and dimensions of the cross section.

The shapes and dimensions of the specimens used are as shown in Fig. 5, and the shapes of the cross section of those specimens are shown in Fig. 6. The fact that the height of cross section for all the shapes of specimens was uniformly set at 12 mm was for the purpose eliminating the effect of apparent stress gradient* on the fatigue limit.

These specimens were produced from 26 mm-dia. rolled bars, and finished by emery papers, grade No. 0000, so as to leave polishing scratches parallel to the longitudinal axis of the specimen. Then they were annealed in vacuum as shown in Table 2 and finally they were once more polished by emery papers, grade No. 0000. Therefore, it is conceivable that each specimen, in the pre-experimental condition, neither is affected by the residual stress and cold-working by machining nor by the direction of polishing scratches**.

The experiments were carried out on the Nishihara's combined bending and torsional fatigue testing machine, and the number of cycles per minute was about 1400.

Data of the experimental results for various kinds of shapes of cross section are summarized in Tables 3 and 4, and those S–N diagrams are shown in Figs. 7 and

* The "apparent" stress gradient implies such a stress gradient as is calculated from the theory of elasticity for the perfectly elastic material.

** Manufacturing methods of specimens can be considered as a possible factor to effect the experimental results of the present problem. Therefore, such a great carefulness was paid in order to eliminate any other effect on the shape effect.

Table 3. Results of flexural bending fatigue tests for 5695.

| Shape of Cross Section | Reversed Stress, $\sigma$ kg/mm$^2$ | Number of Repetitions, N in $10^6$ | Remarks |
|---|---|---|---|
| Rectangular | 20.8 | 2.01 | broken |
| | 17.8 | 0.80 | " |
| | 17.2 | 7.40 | " |
| | 16.5 | 11.23 | not broken |
| I-Shape | 15.7 | 1.50 | broken |
| | 15.2 | 0.75 | " |
| | 14.9 | 6.50 | " |
| | 14.8 | 8.80 | " |
| | 13.5 | 10.14 | not broken |

Table 4. Results of flexural bending fatigue tests for 251.

| Shape of Cross Section | Reversed Stress, $\sigma$ kg/mm$^2$ | Number of Repetitions, N in $10^6$ | Remarks |
|---|---|---|---|
| Round | 25.0 | 6.21 | broken |
| | 22.4 | 4.95 | " |
| | 20.8 | 5.99 | " |
| | 20.4 | 10.00 | not broken |
| | 19.8 | " | " |
| | 19.3 | " | " |
| Rectangular | 25.0 | 0.98 | broken |
| | 22.9 | 2.13 | " |
| | 20.9 | 2.63 | " |
| | 20.4 | 9.73 | " |
| | 19.8 | 10.00 | not broken |
| | 19.3 | " | " |
| I-Shape | 23.0 | 0.296 | broken |
| | 19.8 | 4.20 | " |
| | 19.5 | 2.04 | " |
| | 19.0 | 5.01 | " |
| | 18.7 | 10.00 | not broken |
| | 18.4 | " | " |
| Cross-Shape | 23.0 | 0.296 | broken |
| | 20.5 | 3.06 | " |
| | 20.4 | 2.88 | " |
| | 20.0 | 10.00 | not broken |
| | 19.5 | " | " |
| Tubular | 23.7 | 0.660 | broken |
| | 21.5 | 1.32 | " |
| | 20.0 | 2.10 | " |
| | 19.7 | 10.00 | not broken |
| | 19.5 | " | " |
| | 19.4 | " | " |

Table 5. Bending fatigue limits of specimens with various shapes of cross-section (5695)

| Shape of Cross-Section | Bending Fatigue Limit, kg/mm² |
|---|---|
| Rectangular | 16.8 |
| I-Shape | 14.7 |

Table 6. Bending fatigue limits of specimens with various shapes of cross-section (251)

| Shape of Cross-Section | Bending Fatigue Limit, kg/mm | Ratio for Rectangular Shape | |
|---|---|---|---|
| | | Experiment | Calculation |
| Rectangular | 19.8 | 1.00 | 1.00 |
| Round | 20.4 | 1.03 | 1.05 |
| I-Shape | 18.7 | 0.94 | 0.97 |
| Cross-Shape | 20.0 | 1.01 | 1.04 |
| Tubular | 19.7 | 0.99 | 0.99 |

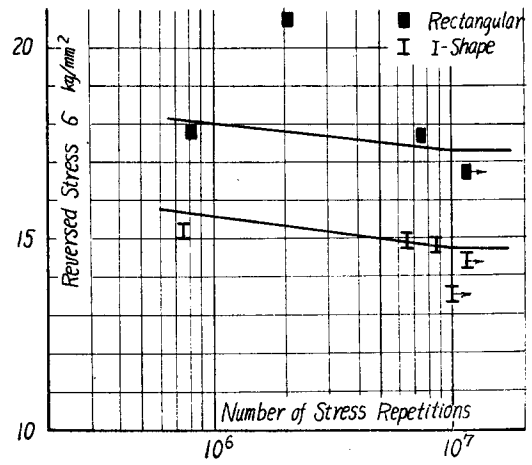


Fig. 7. S-N diagram for 5695.

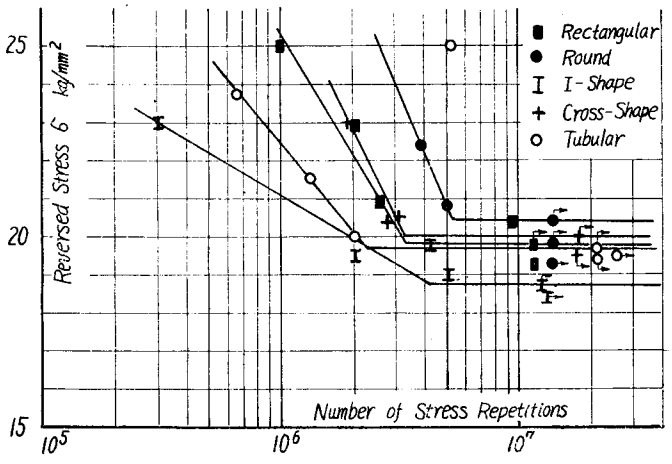


Fig. 8. S-N diagram for 251.

8. And Tables 5 and 6 represent the comparison of the bending fatigue limits for each section obtained from the results.

Although only two types of tests, the rectangular and I-shape, have been conducted on the material 5695, a difference has been clearly recognized between their bending fatigue limits. While, in the case of the material 251 in Table 6, it is clearly shown that the bending fatigue limit is influenced by the shape of cross section, and the maximum fatigue limit is reached on the round specimens while the minimum, on the I-shape specimens.

As it is seen in Figs. 7 and 8, the magnitude of the number of stress repetitions up to the fatigue fracture at the same stress level is also greatest in the round specimens and it becomes smaller in accordance with the magnitude of fatigue limit.

Now that the fatigue limits for various shapes of cross section have been obtained, let us now compare those experimental results with the results derived theoretically in the section 2 of this chapter. The comparison will be made of the experimental results on 251, because only two tests have been performed on 5695.

The bending fatigue limit for each specimen shown in Table 6 can be calculated from Eqs. (9)～(13) by using of the tension-compression fatigue limit $\sigma_w$. However, in this experiment the tension-compression test has not been carried out and the magnitude of $\sigma_w$ is not known. Therefore, the bending fatigue limit of each shape will be shown by comparison to that of the rectangular shape. The 4 th column in Table 6 represents the ratios of fatigue limit to that of rectangular cross section, calculated from Eqs. (9)～(13) by taking $\kappa=0.9$ and $E/E'=2$. Comparing these ratios with those in the 3rd column found from experiments, a perfect agreement is shown in the general tendency, although no perfect coincidence is seen quantitatively. In fatigue tests some extent of error obviously exists in determining fatigue limits and, since the difference between the experimental results and the calculated results shown in Table 6 is in the range of such a experimental error, the theoretical consideration by the authors may well be considered proper so long as they are qualitatively consistent. In other words, it can be said that the authors' theoretical conception described in the chapter 2 is appropriate in discussing the effect of shape of cross section on the fatigue limit.

Next let us make critical reviews of the previous hypotheses on the basis of authors' experimental results.

(1) Hypotheses which take the fracture below surface into consideration. .....By this hypotheses it is considered that the occurrence of fatigue fracture is caused not only by the stress at the surface but also by the stress in a range from the surface and, depending upon how the range is taken, it is divided into the following two cases; in one case, the range is taken as a length to a distant point below the surface; and in the other, as an area to a distant depth. These hypotheses are applied in explaining the notch sensitivity or the size effect and it is said that they adequately explain the experimental results. However, in the former hypothesis, there will be no difference among the bending fatigue limits of various shapes of cross section in case these experiments are performed under the same stress gradient for each specimen. Also, in the latter hypothesis, the difference between the fatigue limits of round and rectangular specimens can be explained, but for the other shapes, interpretation cannot be made adequately unless a considerably large depths are taken. However, since the fatigue fracture arises from a successive development of local failures, it is improper to consider of too large a range. By these reasons, these hypotheses fail to give adequate answers to the present problems.

(2) Hypothesis based on a statistical viewpoint. ……This is a hypothesis which is formed on the consideration that the material generally contains many a defect, such as non-metallic inclusion, segregation and others and it is never homogeneous, and it explains to some extent the effect of shape. This hypothesis has it that between the round shape and the rectangular shape, the portion that receives the greatest stress is smaller in the case of the former, and compared with the latter, the bending fatigue limit is greater. However, in this experiment, since the fatigue limits of specimen with the rectangular and I-shape cross section differ from each other in spite of the same breadth, this hypothesis is not satisfactory for the explanation of fatigue fracture.

Thus, comparison has been made of these previous hypotheses with the experimental results that the authors obtained, but none of them can give sufficient explanations.

3.2 Experimental results by the other investigators and the consideration

Little experiments have been done in regard to the shape effect of cross section of specimen on the fatigue limit. On comparison of the bending fatigue limits, for example, none has likely been made for various shapes, as have been conducted by the authors. Therefore, as many experimental results capable of comparison with the authors' theoretical consideration as possible will be described in the following discussion.

(1) Comparison between the respective bending fatigue limits of round and rectangular specimens. .....Dolan[13] carried out tests for two materials with four kinds of shape of cross section, namely; round, square, diamond and modified diamond. However, since there seems to be further questions regarding the results for the diamond and modified diamond specimens, let us here consider the results for the round and rectangular specimens. Table 7 shows his results. Fig. 9 represents a relation between $E/E'$ and $\sigma'_{w\bullet}/\sigma'_{w\blacksquare}$ when $\kappa=0.9$. Comparing the experimental results listed in Table 7 with the theoretical results shown in Fig. 9, it is clear that the respective values of

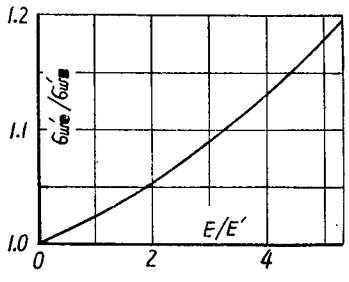


Fig. 9. Relation between $\sigma'_{w\bullet}/\sigma'_{w\blacksquare}$ and $E/E'$.

Table 7. Comparison between the flexural bending fatigue limits of round and rectangular specimens (Dolan).

| Material | Carbon Content, % | Yield Point, kg/mm² | Tensile Strength, kg/mm² | Flexural Bending Fatigue Limit, kg/mm² | | $\sigma'_{w\bullet}/\sigma'_{w\blacksquare}$ | $E/E'$ |
|---|---|---|---|---|---|---|---|
| | | | | Round $\sigma'_{w\bullet}$ | Rectangular $\sigma'_{w\blacksquare}$ | | |
| SAE 4340 | 0.39 | 100.0 | 105.7 | 63.6 | 56.6 | 1.124 | 3.9 |
| Mayari $R$ | 0.10 | 37.0 | 52.9 | 35.2 | 32.3 | 1.087 | 3.0 |

$E/E'$ listed in the last column of Table 7 serves good agreement. And these values for $E/E'$, in accordance with the discussion carried in the section 4 of chapter 1, are in general appropriate for the type of steel. In other words, what the authors consider gives adequate explanation to Dolan's experimental results.

(2) Comparison of the rotating bending fatigue limit of round specimen with the flexural bending fatigue limit of rectangular specimen. .....Moore[10] carried out fatigue tests on various kinds of carbon steels having 0.02~1.2% carbon contents and special steels, and obtained the ratio of the rotating bending fatigue limit of round section, $\sigma''_{w\bullet}$, to the flexural bending fatigue of rectangular section, $\sigma'_{w\blacksquare}$. These results are shown in Fig. 10, in which the abscissa denotes $\sigma''_{w\bullet}$ and the ordinate $\sigma''_{w\bullet}/\sigma'_{w\blacksquare}$. From the figure, it can be seen that, as a general trend, $\sigma''_{w\bullet}/\sigma'_{w\blacksquare}$ becomes larger as $\sigma''_{w\bullet}$ becomes larger, that is, it becomes larger in case of materials containing higher carbon contents.

According to the authors' conception, since the values of $E/E'$ becomes generally smaller in the steels of higher carbon contents, the above results are seen to be quite contrary. This seems to be due to inadequacy of specimens used by Moore. That is, the shapes of specimens used by Moore as shown in Fig. 11 and, although there is no questions pertaining to the specimens for the rotating bending test, in case of

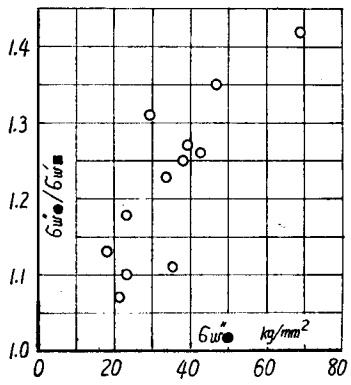


Fig. 10. Relation between $\sigma''_{w\bullet}/\sigma'_{w\blacksquare}$ and $\sigma''_{w\bullet}$ (Moore).

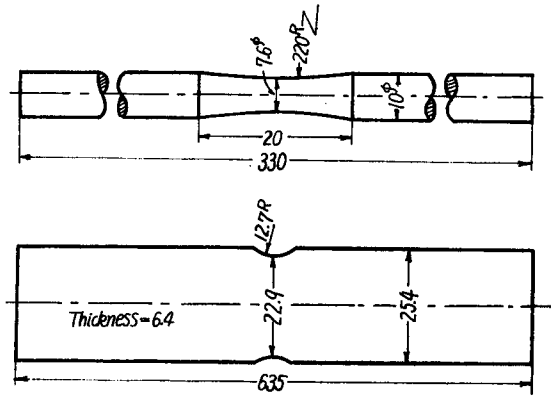


Fig. 11. Shapes of specimens used by Moore.

the flexural bending specimen of rectangular section the stress concentration is likely to take place at both sides of critical section due to improper selection of the shapes of specimen. Moreover, since the notch effect caused by this stress concentration is greater in the material with larger $\sigma''_{w\bullet}$, $\sigma'_{w\blacksquare}$ becomes smaller than it is in the case without such stress concentration. Thus, it seems that $\sigma''_{w\bullet}/\sigma'_{w\blacksquare}$ became greater with the magnitude of $\sigma''_{w\bullet}$ expanded. Therefore, excepting the experimental results for the material whose $\sigma''_{w\bullet}$ is over 25 kg/mm² and calculating an average value of $\sigma''_{w\bullet}/\sigma'_{w\blacksquare}$ from the experimental results for four kinds of materials, the following relation holds,

$$\sigma''_{w\bullet}/\sigma'_{w\blacksquare} = 1.12\,.$$

Then, taking about 3.8 as $E/E'$ from Fig. 9, good coincidence is seen with the experimental results.

(3) Comparison between the tension-compression fatigue limit and rotating bending fatigue limit.....This series of experiments have been committed by Gough[14], France[15], Swanger[16], Nishihara[17] and the others, and the results obtained by them are summarized in Table 8. It can be seen from the table that the rotating bending fatigue limit $\sigma''_{w\bullet}$ is greater than that of the tensioncompression, $\sigma_w$.

Table 8. Values of $\sigma''_{w\bullet}/\sigma_w$ for various materials.

| Investigator | Carbon Content, % | Heat Treatment | $\sigma''_{w\bullet}/\sigma_w$ |
|---|---|---|---|
| R. D. France | 0.45 | Annealed | 1.35 |
| " | " | Quenched and tempered | 1.01 |
| " | 0.47 | Annealed | 1.25 |
| " | " | Quenched and tempered | 1.18 |
| " | 0.87 | Annealed | 1.33 |
| " | " | Quenched and tempered | 1.00 |
| H. J. Gough | 0.48 | Cold-rolled | 1.14 |
| W. H. Swanger | 0.02 | Cold-rolled | 1.04 |
| " | 0.45 | Annealed | 1.41 |
| " | " | Quenched and tempered | 1.01 |
| " | 0.72 | Annealed | 1.20 |
| " | " | Quenched and tempered | 1.52 |
| T. Nishihara | 0.44 | As-received | 1.21 |
| " | 0.60 | " | 1.26 |
| " | 0.65 | " | 1.17 |

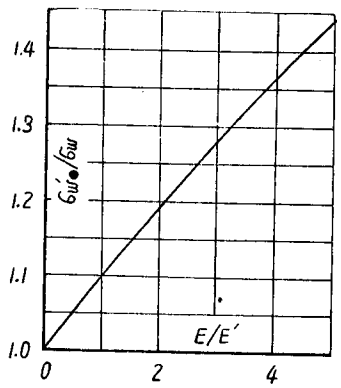


Fig. 12. Relation between $\sigma'_{w\bullet}/\sigma_w$ and $E/E'$.

On the other hand, taking 0.9 as $\kappa$ in Eq. (10) obtained by the authors and calculating the relation between $\sigma'_{w\bullet}/\sigma_w$ and $E/E'$, Fig. 12 is obtained. Comparing the calculated results with the experimental results, good agreement is seen in the range of $E/E'=0\sim4$. Further, the value of $\sigma''_{w\bullet}/\sigma_w$ is smaller in the steel of higher carbon contents and in the qenched and tempered state than in annealed state. These materials are of more notch sensitivity and necessarily have smaller value of $E/E'$, therefore, it is obvious that $\sigma''_{w\bullet}/\sigma_w$ becomes smaller.

(4) Comparison of the torsional fatigue limit

of solid specimen with that of tubular specimen.....Gough[11] carried out the comparison tests of torsional fatigue limits for two kinds of specimens, that is, solid and tubular specimens having the ratio of inner diameter to outer diameter of 0.782. Table 9

Table 9. Comparison between the torsional fatigue limits of solid and tubular specimens (Gough).

| Material | Torsional Fatigue Limit, kg/mm² | | Ratio of Torsional Fatigue Limits, Tubular/Solid |
|---|---|---|---|
| | Tubular | Solid | |
| Low Carbon Steel | 13.4 | 16.5 | 0.808 |
| Medium Carbon Steel | 14.0 | 15.9 | 0.881 |

represents the results and demonstrates that the ratio of both fatigue limits becomes smaller as the carbon contents become lower. Comparing the results with the authors' results shown in Fig. 4, for the medium carbon steel they coincide well when $\kappa=0.9$, $G/G'=8$, but for the low carbon steel $G/G'$ must be taken as a larger value than 2.

(5) Magnitude of the fatigued portion.....One of the authors[9] have detected the magnitude of fatigued portion, by a corrosion method, which takes place in various reversed stress levels under rotating bending and torsion tests. In the tests, the amounts of elastic portion, excluding the fatigued portion, in the case of fatigue limit for the reversed stress in each test were as follows;

$$x_p/h \cong 0.7 \quad \text{for rotating bending,}$$
$$r_p/R \cong 0.5 \quad \text{for reversed torsion,}$$

where $x_p$ or $r_p$ denotes a distance from the center of specimen to a boundary point between the elastic and fatigued portions, and $h$ or $R$ is the radius of each specimen.

According to the authors' consideration, $x_p/h$ in Fig. 2 is equivalent to $x_p/h$ or $r_p/R$ in the above experiments, and then these values can be expressed by $\kappa$, $E/E'$ or $G/G'$ as follows,

$$\frac{x_p}{h}=\frac{\sigma_p}{E\varepsilon_w}=\kappa\Big/\left\{1+\frac{E}{E'}(1-\kappa)\right\} \quad \text{for rotating bending,}$$
$$\frac{r_p}{R}=\frac{\tau_p}{G\gamma_w}=\kappa\Big/\left\{1+\frac{G}{G'}(1-\kappa)\right\} \quad \text{for reversed torsion.}$$

Therefore, substituting $E/E'=3$, $G/G'=8$, $\kappa=0.9$, the amounts of fatigued portion obtained for the respective cases agree with those of the above experimental results. And the values of $E/E'$ and $G/G'$ adopted here for the mild steel are considered proper.

As described above, according to the authors' conception, the amount of fatigued portion also can be determined and further it is clear that the amount of fatigued portion varies with the kind of material.

### 4. Conclusions

The following is the summary of conclusion reached as the results of this investigation:

(1) The flexural bending fatigue tests were carried out on specimens having five kinds of cross section — round, cross-shape, rectangular, tubular and I-shape —, and it became known that the fatigue limits for respective sections become smaller in the order of shapes of cross section, given above.

(2) The fact that the flexural fatigue limit differs depending upon the shape of cross section, which has been made clear by the above experimental results, can be rationally explained by taking into consideration the phenomenon of elastic hysteresis which appears between stress and strain during fatigue tests.

(3) Under the same consideration, the relation between the tension-compression fatigue limit and the bending fatigue limit can be made clear, and also the amount of fatigued portion can be known by the calculation. The results obtained from the calculation showed good coincidence with the experimental results.

## Chapter 3. On the Relation between the Form Factor and the Notch Factor

### 1. Introduction

It has been recognized by many investigations that the notch factor is generally less than the form factor. And many a conception such as the followings have been offered pertaining to the explanation of the above fact; the Neuber's formula[18] which takes into consideration the size of elementary structure unit, the effect of stress gradient at the peak stress[19], the discussion based on the average stress in some range between the surface and an inner point[20], a statistical consideration[21] and others[22]. However, since the phenomenon of elastic hysteresis takes place in faigue tests as mentioned above, henceforth the actual peak stress at the root of the notch is obviously less than that obtained by the calculation of elasticity. In this chapter, the authors attempted to derive theoretically the relation between the form factor and notch factor under consideration of the phenomenon of elastic hysteresis and compared the derived results with the authors' experimental results.

### 2. Theoretical consideration on the relation between the form factor and notch factor

If the notched specimen is subjected to a reversed stress near or over the fatigue limit, the phenomenon of elastic hysteresis appears near the root of the notch as mentioned before. When the material prior to fatigue tests is considered to be perfectly elastic, the peak stress $\alpha\sigma_n$ (i.e. $\alpha$ is the form factor and $\sigma_n$, the nominal stress) is thought to appear at the root of the notch. However, when the fatigued

portion appears near the root of the notch under reversed stress, it is no longer considered to have produced the stress $\alpha\sigma_n$ at the root of the notch. Only the smaller stress appears due to the elastic hysteresis loop being formed.

It is a matter of course, therefore, that the notch factor becomes necessarily smaller than the form factor and, by developing this consideration, the relation between the form factor and notch factor can be quantitatively determined.

In the subsequent discussion, the case of a specimen with a deep hypaboloid groove as shown in Fig. 13 subjected to the reversed torsion, will be explained for the convenience of the forthcoming comparison with the experimental results. In such a case, only a shear stress $\tau$ exists at the critical section of root of the notch at which the fatigue fracture may occur, and the other stresses do not exist. Consequently, for the condition of fatigue limit in this case, Eq. (6), as it is, can be applied and it is construed that, when the shearing strain at the root of the notch becomes equal to $\gamma_w$, the fatigue limit is reached. Therefore, calculating the torsional moment due to the stress distribution at the critical section and dividing the moment by the sectional coefficient, the apparent fatigue limit, that is, the fatigue limit which is conventionally obtained, can be determined. In this case, however, in order to accurately calculate the torsional moment, the accurate stress distribution within the section must be known, but it is very difficult because the portion near the root of the notch is being fatigued. Fortunately, however, the fatigued portion appears only locally near the root and, even if the stress distribution may vary from the original elastic distribution, the distribution of shearing strain may well be considered, by approximation, similar to the strain when the entire cross section is perfectly elastic. In other words, we consider it as the distribution of strain when the strain at the root of the notch elastically becomes $\gamma_w$. So the torsional moment can be calculated comparatively simply by this method.

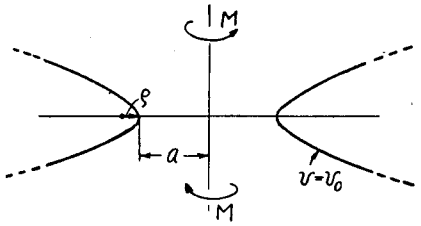

Fig. 13. Deep V-grooved notch.

Now, the distribution of shearing stress $\tau$ at the section of root of the notch when the deep notch, as shown in Fig. 13, is subjected to elastic torsional moment, is given by Neuber as follows;

$$\tau = \frac{3}{4} p \frac{\sin v_0(1+\cos v_0)}{(2+\cos v_0)(1-\cos v_0)} \tan v, \tag{17}$$

where $p$ is the nominal stress, $\sin v_0$ and $\cos v_0$ are the values calculated from the following equations by using the radius of the section, $a$, and the notch radius $\rho$,

$$\sin v_0 = \sqrt{\frac{a/\rho}{a/\rho+1}}, \quad \cos v_0 = \frac{1}{\sqrt{a/\rho+1}}. \tag{18}$$

Therefore, the interior strain distribution corresponding the elastic strain at the surface of critical section, $\gamma_w$, can be found from the stress distribution when $\tau=G\gamma_w$ for $v=v_0$ in Eq. (17). And $G\gamma_w$ is the value obtained by substituting Eq. (6) into $\gamma_w$ as follows:

$$G\gamma_w = \tau_0 = \left\{1+\frac{G}{G'}(1-\kappa)\right\}\tau_w, \tag{19}$$

where $\tau_w$ is the torsional fatigue limit of ideally thin-walled tubular specimen. Consequently, substituting $\tau_0$ in Eq. (19) for $\tau$ in Eq. (17) and putting $v=v_0$, the nominal stress $p_n$ at the above stress distribution becomes

$$p_n = \frac{4}{3}\frac{(2+\cos v_0)(1-\cos v_0)}{\sin v_0(1+\cos v_0)\tan v_0}\tau_0. \tag{20}$$

Therefore, putting this $p_n$ into Eq. (17) and dividing by $G$, the interior strain distribution corresponding to the surface strain $\gamma_w$ can be obtained. That is:

$$\gamma = \frac{\tau_0}{G\tan v_0}\tan v. \tag{21}$$

Further, $v_e$, the value of $v$ which shows the boundary between the fatigued and elastic portions, can be obtained from the condition that the stress at the boundary must be equal to $\kappa\tau_w$. Thus:

$$v_e = \tan^{-1}\frac{4}{3}\frac{\kappa\tau_w(2+\cos v_0)(1-\cos v_0)}{p_n\sin v_0(1+\cos v_0)} = \tan^{-1}\kappa\frac{\tan v_0}{\tau_0}\tau_w. \tag{22}$$

Since the relative magnitudes of fatigued and of elastic portions and the interior strain distribution were clarified in the above, now the stress distribution can be obtained by applying Eq. (5) to the fatigued portion ($v\geq v_e$) and the usual elastic formula $\tau=G\gamma$ to the elastic portion. To obtain the torsional moment $M_T$ from the above, the equation becomes as follows:

$$M_T = \frac{\pi}{2}p_n\frac{\sin v_0(1+\cos v_0)}{(2+\cos v_0)(1-\cos v_0)}\left[(2+\cos v_e)(1-\cos v_e)^2+\frac{1}{1+G/G'}(\cos^3 v_0-3\cos v_0 - \cos^3 v_e+3\cos v_e)\right]+\frac{2\pi}{3}\frac{\kappa\tau_w}{1+G'/G}(\sin^3 v_0-\sin^3 v_e). \tag{23}$$

Calculating the nominal stress $\tau_n$ from the above $M_T$, it becomes:

$$\tau_n = 2M_T/\pi\sin^3 v_0, \tag{24}$$

and the notch factor $\beta$ can be obtained by:

$$\beta = \tau_{w\bullet}/\tau_n, \tag{25}$$

where $\tau_{w\bullet}$ is the torsional fatigue limit of unnotched specimens whose diameter is equal to that of the critical section of notched specimen.

In order to perform the above calculation, it is necessary to seek the torsional fatigue limit of ideally thin-walled tubular specimen, $\tau_w$, but, from the practical point of view, it is impossible to obtain the accurate magnitude of $\tau_w$. Therefore, using Eq. (14) and expressing $\tau_w$ with $\tau_{w\bullet}$ and substituting in Eq. (25), $\beta$ becomes as follows:

$$\beta=\frac{3}{4}\sin^3 v_0\left[1+\frac{1}{3}\frac{\kappa}{1+\frac{G'}{G}}-\frac{1}{3}\frac{1}{1+\frac{G'}{G}}\frac{\kappa^4}{\left\{1+\frac{G}{G'}(1-\kappa)\right\}^3}\right]\Bigg/\left[\frac{1+\frac{G}{G'}(1-\kappa)}{\tan v_0}\{(2+\cos v_0)\times\right.$$

$$\left.(1-\cos v_e)^2+\frac{1}{1+\frac{G}{G'}}(\cos^3 v_0-3\cos v_0-\cos^3 v_e+3\cos v_e)\}+\frac{\kappa}{1+\frac{G'}{G}}(\sin^3 v_0-\sin^3 v_e)\right]. \quad (26)$$

As seen in Eq. (26), $\tau_{w\bullet}$ is not included in the equation, and it shows that the notch factor $\beta$ can only be calculated from $G/G'$ and $\kappa$. This goes to show the fact that $\beta$ varies depending upon materials even for the same value of $\alpha$ is due to the magnitude of elastic hysteresis loop which occurs during the fatigue test of the material.

Fig. 14 shows the relation between the form factor $\alpha$ and notch factor $\beta$ calculated from Eq. (26) for the various values of $G/G'$ when $\kappa=0.9$. As seen in the figure, $\beta$ becomes smaller with the increase of $G/G'$ and so the difference with $\alpha$, which was theoretically obtained by Neuber, becomes larger.

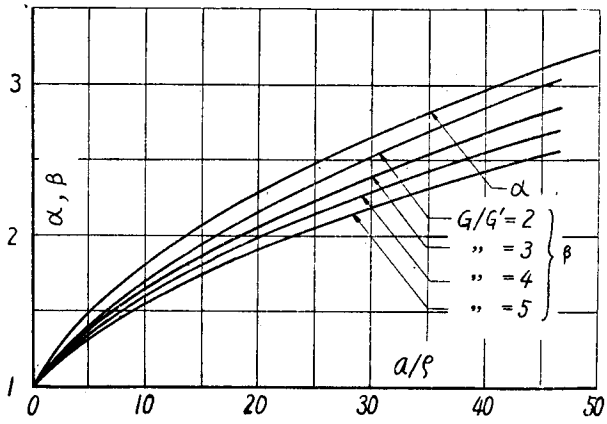


Fig. 14. Relation between the form factor $\alpha$ and the notch factor $\beta$.

In the above, the procedure of finding theoretically the relation between the form factor and notch factor when the notched specimen, as shown in Fig. 13, is subjected to the reversed torsional stress has been made clear.

The similar procedure is applicable for the plane notch in which the stress at the surface of the root of the notch is one-dimensional. But in the case of bending of the specimen with the three-dimensional notch, we must modify the condition of the fatigue limit, because the stress at the root of the notch becomes two-dimensional. However, the stress perpendicular to the surface vanishes at the surface in every case, so it suffices to consider the cases of two-dimensional stress as the condition of the fatigue limit. We shall report on this case in the later treatise.

Table 10. Chemical composition of materials (%).

| Mark | C | Mn | Si | P | S |
|---|---|---|---|---|---|
| 5637 | 0.10 | 0.62 | 0.16 | 0.044 | 0.040 |
| 987 | 0.65 | 0.62 | 0.20 | 0.020 | 0.031 |

## 3. Materials tested and specimens

The materials used in this experiment are of two kinds of carbon steels and their chemical compositions and mechanical properties are listed in Table 10 and 11.

Table 11. Mechanical properties of materials.

| Mark | Heat Treatment | Yield Point, kg/mm² | Tensile Strength, kg/mm² | Breaking Strength on Final Area, kg/mm² | Elongation, % | Reduction of Area, % | Hardness, Shore | Torsional Yield Point, kg/mm² | Torsional Breaking Strength, kg/mm² |
|---|---|---|---|---|---|---|---|---|---|
| 5637 | Heated at 910°C for 1 hr. in vacuum, then cooled in furnace. | $\sigma_{s0}$=26.9<br>$\sigma_{su}$=22.1 | 41.1 | 84.3 | 37.1 | 58.1 | 14.8 | $\tau_{s0}$=18.2<br>$\tau_{su}$=16.5 | 48.5 |
| 987 | Heated at 830°C for 1 hr. in vacuum, then cooled in furnace. | $\sigma_{s0.2}$=31.7 | 75.4 | 92.2 | 12.2 | 36.5 | 24.1 | $\tau_{s0.2}$=21.6 | 68.2 |

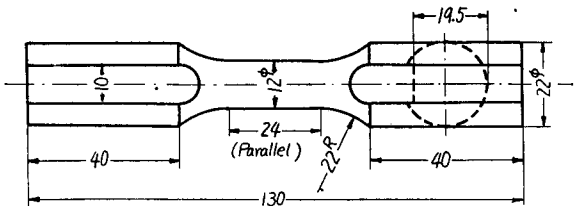


(unnotched Specimen)

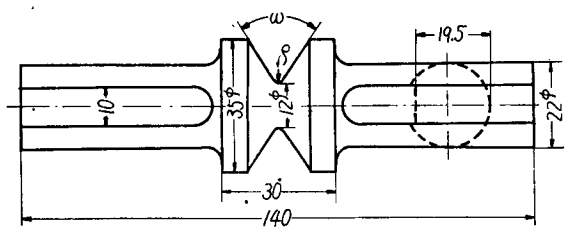


(Notched Specimen)

Fig. 15. Shapes of specimens.

Table 12. Dimensions of fatigue specimens.

| Mark | 5 637 | | | 987 | | | |
|---|---|---|---|---|---|---|---|
| $\rho$ mm | ∞ | 1.22 | 0.23 | ∞ | 1.22 | 0.47 | 0.15 |
| $\omega$° | 180 | 60 | 36 | 180 | 60 | 36 | 28 |
| a/$\rho$ | 0 | 4.92 | 25.69 | 0 | 4.92 | 12.77 | 40.82 |
| $\alpha$ | 1.00 | 1.50 | 2.52 | 1.00 | 1.50 | 1.98 | 3.00 |

The shapes of specimens employed are shown in Fig. 15. For the notched specimen in the figure, the depth of notch and the diameter at the critical section $2a$ were maintained constant, but the notch radius $\rho$ were varied two or three kinds throughout this experiments. The notch angle was also varied in accordance with the magnitude of $\rho$ as shown in Table 12. The reason was that in the preceeding section, the relation between $\alpha$ and $\beta$ was obtained by partial application of the Neuber's theory, so that the shape of specimen, which is applicable for the theory, i.e. the hypaboloid notch, must be chosen.

However, in such a magnitude of $\rho$ as used here, the

V-grooved notch with the notch angle $\omega$ that corresponds to each magnitude of $\rho$, as shown in Table 12, has no appreciable difference from the hypaboloid notch; therefore, for the convenience of manufacturing, the V-grooved notches were chosen.

Further, the Neuber's theory gives the exact value of form factor only in the extreme cases of very deep or very shallow notch but is quite inaccurate in the cases of optional depths. Besides, the distribution of interior stress cannot be obtained. Therefore, a specially large depth of notch was selected as shown in Fig. 15 in order that the notch may be regarded as a very deep one.

The form factor $\alpha$ in Table 12 is obtained from the Neuber's formula for the case of very deep notch and when it is compared with the value obtained form his combined formula, the difference falls within the range of from 1 to 2%. Thus it may well be considered that the specimens used in this test have very deep notch. Moreover, after these specimens were produced, they were heat treated as shown in Table 11 in order to avoid the effect of machining operation. After that, the specimens were polished with the emery paper, No. 0000, at and near the root of the notch.

These tests were carried out with the Nishihara's torsional fatigue testing machine, and the number of cycles per minute was about 3000.

### 4. Experimental results and the consideration

In the reversed torsion tests of unnotched specimens, if a crack occurs at the surface, the crack develops rapidly and the specimen is caused to fracture after small number of stress repetitions and there is no case in which the specimen does not fracture despite the occurrence of crack.

In the notched specimen, however, the more the notch becomes sharp, the greater becomes the number of stress repetitions from the occurrence of crack until the fracture. And, in the case of very sharp notches, the crack does not grow even though it may appear at the root of the notch. In these tests, there were many cases in which the specimen endured for considerably large number of stress repetitions after the occurrence of crack, or those which did not fracture even with number of stress repetitions $10^7$. In the conventional method of determining the fatigue limit with the unnotched specimen the method of finding the maximum reversed stress at which the specimen did not fracture was used. In such case, it is proper to consider the maximum reversed stress as the fatigue limit because the crack at the surface, i.e. the portion with the maximum stress, always accompanies the fracture of specimen. On the contrary, in the notched specimen, the occurrence of crack at the peak stress is not always followed by fracture of specimens. However, from the practical point of view, it may be advisable to call the maximum stress at which the specimen does not rupture the fatigue limit. However, when a consideration is being made of the notch factor in relation to the form factor, as in this study, the occurrence of crack

at the root of the notch must be regarded as the fatigue fracture even though the crack may not grow. Consequently, the maximum stress at which the fatigue crack do not occur ought to be defined as the fatigue limit of the notched specimen, and for the purpose of determining the fatigue limit as above, the fatigue crack which appears at the root of the notch must be detected. But the crack is so minute that the detection by the naked eye is very difficult and the detection of crack in this experiment was made with the microscope having 30 times magnification.

Tables 13 and 14 represent the experimental results for each material by the

Table 13. Results of fatigue tests for 5637.

| Dimension of Notch, $a/\rho$ | Reversed Stress, $\tau$ kg/mm$^2$ | Remarks | Torsional Fatigue Limit, kg/mm$^2$ |
|---|---|---|---|
| 0 | 12.9 | broken | 12.8 |
| " | 12.8 | not broken | |
| " | 11.8 | " | |
| " | 11.2 | " | |
| 4.92 | 9.6 | Cracked | 9.0 |
| " | 9.2 | " | |
| " | 7.9 | not cracked | |
| " | 6.6 | " | |
| 25.69 | 7.5 | broken | 6.0 |
| " | 6.2 | cracked | |
| " | 5.2 | not cracked | |

Table 14. Results of fatigue tests for 987.

| Dimension of Notch, $a/\rho$ | Reversed Stress, $\tau$ kg/mm$^2$ | Remarks | Torsional Fatigue Limit, kg/mm$^2$ |
|---|---|---|---|
| 0 | 15.7 | broken | 15.5 |
| " | 15.3 | not broken | |
| " | 15.2 | " | |
| 4.92 | 12.5 | broken | 11.5 |
| " | 12.2 | " | |
| " | 12.0 | " | |
| " | 11.2 | not cracked | |
| 12.77 | 11.0 | cracked | 9.5 |
| " | 9.9 | " | |
| " | 9.3 | not cracked | |
| " | 9.0 | " | |
| 40.82 | 6.8 | cracked | 6.1 |
| " | 6.0 | " | |
| " | 6.0 | not cracked | |
| " | 5.4 | " | |

method described heretofore. The number of stress repetitions up to fracture for the unnotched specimens (specimens corresponding to $a/\rho=0$ in the tables) was clear; however for the specimens with which the occurrence of crack was tested, the number of stress repetitions just at the point of occurrence was not accurately determined even though the crack did actually occur, so the number is not represented in these tables. For the specimens on which the crack did not occur, the number of stress reversals of $10^7$ was given in all cases.

The values of notch factor $\beta$ for each material obtained from the results are listed in Tables 15 and 16. In addition, the values of $\alpha$ calculated on the assumption of having very deep notches are also represented in these tables.

Table 15. Torsional fatigue limit and the notch factor for 5637.

| Dimension of Notch, $a/\rho$ | Torsional Fatigue Limit, $\tau_w$ kg/mm$^2$ | Form Factor, $\alpha$ | Notch Factor $\beta$, | |
|---|---|---|---|---|
| | | | Experiment | Calculation |
| 0 | 12.8 | 1.00 | 1.00 | 1.00 |
| 4.92 | 9.0 | 1.50 | 1.42 | 1.36 |
| 25.69 | 6.0 | 2.52 | 2.13 | 2.18 |

Table 16. Torsional fatigue limit and the notch factor for 987.

| Dimension of Notch, $a/\rho$ | Torsional Fatigue Limit, $\tau_w$ kg/mm$^2$ | Form Factor, $\alpha$ | Notch Factor $\beta$, | |
|---|---|---|---|---|
| | | | Experiment | Calculation |
| 0 | 15.5 | 1.00 | 1.00 | 1.00 |
| 4.92 | 11.5 | 1.50 | 1.35 | 1.36 |
| 12.77 | 9.5 | 1.98 | 1.64 | 1.73 |
| 40.82 | 6.1 | 3.00 | 2.54 | 2.58 |

By the above, the relation between $\alpha$ and $\beta$ was clarified by tests, so let us now compare these experimental results with the results calculated by the method described in the section 2. For this calculation, Eq. (26) is used for various shapes of notches. Then the values of $G/G'$ and $\kappa$ must be known. Now, taking into account the general characteristics of $G/G'$ which becomes smaller in magnitude as the carbon content increases, we will adopt the following values as being reasonable values:

$G/G'=4.5$, $\kappa=0.9$ for 5637,
„ $=4.0$, „ $=0.9$ for 987.

The magnitudes of $\beta$ calculated for each material with the above values are shown in the 5th column of Tables 15 and 16. Fig. 16 and 17 represent their comparison with the experimental results. As it is seen

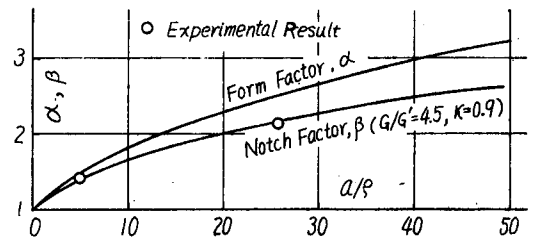


Fig. 16. Comparison between experimental and calculated results for 5637.

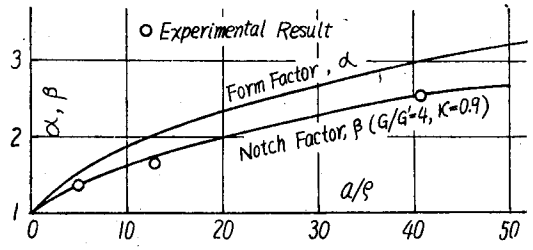


Fig. 17. Comparison between experimental and calculated results for 987.

in the figures, good agreement are shown between those magnitudes of $\beta$ obtained from experiments and those, by calculation. The form factor $\alpha$ in the figures is the one given by Neuber for the deep notch cases.

As mentioned above, it was made clear that the relation between the form factor and the notch factor obtained by the procedure described in the section 2 have good consistency with experimental results. And the authors maintain that the factor that the notch factor is less than the form factor is due to the phenomenon of elastic hysteresis between stress and strain during fatigue tests.

## 4. Conclusions

The following is the summary of conclusion reached as the result of this investigation:

(1) The relation between the form factor and the notch factor was theoretically derived by taking into consideration the phenomenon of elastic hysteresis.

(2) From the torsional fatigue tests of specimens having various sharpness of deep V-grooved notches on two kinds of carbon steels, the relations between the notch factor and sharpness of the notch were obtained. In these tests, particular attention was paid to the determination of fatigue limit, that is, the fatigue limit of notched specimen was decided as the maximum stress at which the crack do not occur at the root of the notch.

(3) Good coincidence was obtained between the experiments and the theoretical consideration.

## Closure

As has been pointed out in Introduction, little attention has been paid to the phenomenon of elastic hysteresis in the case of the discussion of fatigue strength. However, since such a phenomenon has direct bearing upon the substance of fatigue, its consideration cannot be neglected. The authors carried on their studies on this point of view, and tried at first to express the phenomenon with a simple formula by refering to various experimental results of the past and subsequently gave the condition of fatigue limit with the strain. By using such expressions, the effect of shape of cross section of specimen on the fatigue limit and the relation between the form factor and the notch factor were theoretically treated and were compared with the experimental results of the authors as well as of other investigators. The results

derived theoretically had good coincidence with the experimental results, and it was established that the consideration of the phenomenon of elastic hysteresis is very important in the discussion of fatigue strength.

**References**


1) L. Bairstow, Roy. Soc. London, Phil. Trans., p. 210 (1910).
2) W. Mason, Instn. Mech. Engr., J. p. 121 (1917).
3) Z. Nagasawa, Japan Soc. Mech. Engr., J., Vol. 31, p. 259 (1928).
4) S. Dorey, Instn. Mech. Engr., Proc., Vol. 123, p. 479 (1932).
5) B. J. Lazan & T. Wu, Amer. Soc. Testing Mat., Proc., Vol. 51, p. 649 (1951).
6) G. R. Brophy, Amer. Soc. Tetals, Trans., Vol. 24, p. 154 (1936).
7) E. Kaufmann, Über die Dauerbiegefestikeit einiger Eisenwerkstoffe und ihre Beeinflussung durch Temperatur und Kerbwirkung, Berlin, Springer, 1931.
8) M. Kikukawa, Japan Soc. Mech. Engr., Trans., Vol. 7, No. 28 (1941).
9) T. Nishihara & M. Kawamoto, Mem. Coll. Eng. Kyoto Jap. Univ., Vol. 11 No. 3, p. 31 (1943).
10) H. F. Moore, Univ. Illinois, Bull., No. 142 (1924).
11) H. J. Gough, The Fatigue of Metals, p. 99 (1926).
12) F. B. Fuller & T. T. Oberg, Amer. Soc. Testing Mat., Proc., Vol. 47, p. 665 (1947).
13) T. J. Dolan, J. H. Mc Clow & W. J. Craig, Amer. Soc. Mech. Engr., Trans., Vol. , p. 469 (1950).
14) H. J. Gough & J. Tapsell, Aeron. Res. Comm., R. & M., No. 1012 (1926).
15) R. D. France, Amer. Soc. Testing Mat., Proc., Vol. 31, p. 176 (1931).
16) W. H. Swanger & R. D. France, Amer, Soc. Testing Mat., Proc., Vol. 32, p. 432 (1932).
17) T. Nishihara, Japan Soc. Mech. Engr., J., Vol. 39, p. 436 (1936).
18) H. Neuber, Kerbspannungslehre, s. 90 (1937).
19) R. E. Peterson, Stephen Timoshenko Sixtieth Anniversary Volume, p. 179 (1938).
20) R. E. Peterson, Exp. Stress Analysis, Proc., Vol. 1, p. 118 (1943).
21) N. N. Aphansiev., Engineer's Digest, Vol. 5, No. 3 (1948).
22) C. S. Yen & T. J. Dolan, Univ. Illinois, Bull., No. 398 (1952).